Progress In Electromagnetics Research, Vol. 116, 395–408, 2011

DESIGN AND SIMULATION OF L-SHAPED CHIRAL NEGATIVE REFRACTIVE INDEX STRUCTURE

J. Li, F.-Q. Yang, and J.-F. Dong*

Institute of Optical Fiber Communication and Network Technology
Ningbo University, Ningbo 315211, China

Abstract—A new L-shaped chiral structure working in microwave and optical frequency bands has been designed and simulated. The circular dichroism, ellipticity angle, polarization azimuth rotation angle, and effective parameters of this structure, including relative permittivity, relative permeability, chiral parameter and refractive index, are retrieved from simulated transmission and reflection spectra. The results show that the exceptionally strong optical activity is found for the L-shaped chiral structure. Because of the large chiral parameter of this structure, negative refractive index of one circularly polarized wave can be obtained without simultaneously negative permittivity and negative permeability.

1. INTRODUCTION

Recently, the negative refractive index media have attracted much attention because they have a series of unique electromagnetic properties such as negative refraction phenomenon, abnormal Cherenkov radiation and reversed Doppler shift, etc. [1]. The methods to achieve negative refractive index, including double-negative approach [2, 3], transmission line (TL) approach [4, 5] and photonic crystal approach [6, 7], have been intensively studied by various research groups. Unlike those methods, Tretyakov et al. [8, 9] and Pendry [10] have discussed the possibility to achieve negative refraction in chiral media.

The chiral media have two important properties. One is called optical activity which characterizes the polarization azimuth rotation angle of elliptically polarized light. The other is circular

Received 26 March 2011, Accepted 6 May 2011, Scheduled 12 May 2011
* Corresponding author: Jian-Feng Dong (dongjianfeng@nbu.edu.cn).

dichroism which is characterized by the difference in transmitted power of the right-handed circularly polarized (RCP) and left-handed circularly polarized (LCP) waves. If the chiral medium has a large chiral parameter, the negative refractive index can be achieved theoretically [11–13].

It is significantly different from double-negative method to achieve negative refractive index in the chiral medium. First, the double-negative method uses two sets of resonant structures for electric and magnetic responses, respectively. Such two structures must resonate in the same frequency range to realize negative refractive index. In the chiral medium, however, only one resonance is required. Second, the chiral medium can realize negative refractive index for one circularly polarized wave, while the double-negative structures possess negative refractive index for the linearly polarized wave [14].

In recent years, theoretical [15–25] and experimental (or simulative) [26–34] studies on chiral negative refractive media have been published in literature. Several chiral negative refractive structures have been proposed, such as cross-wire structure [12, 26], twisted rosettes structure [13, 27, 28], U-shaped structure [29–31], and twisted metallic foil structure [32–34], etc.. In this paper, we design and simulate a new L-shaped chiral structure which owns stronger rotation angle and larger negative refractive index. This chiral structure may have many potential applications such as cloaking [35–37], subwavelength imaging [38–40], focusing [41], optical storage [42], and polarization devices [43, 44], including pure linear polarization rotator and half-wave plate.

2. NEGATIVE REFRACTIVE INDEX IN CHIRAL MEDIA

For isotropic chiral media, the strength of the cross coupling between the magnetic and electric field is characterized by the chiral parameter κ. The constitutive relations in an isotropic chiral medium for a time-harmonic field with $e^{j\omega t}$ are as follows [45]:

$$\mathbf{D} = \varepsilon\varepsilon_0\mathbf{E} - j\kappa\sqrt{\mu_0\varepsilon_0}\mathbf{H}, \quad \mathbf{B} = \mu\mu_0\mathbf{H} + j\kappa\sqrt{\mu_0\varepsilon_0}\mathbf{E}, \tag{1}$$

where ε and μ are the relative permittivity and permeability of the chiral medium respectively, ε_0 and μ_0 are the permittivity and permeability of vacuum. There are two eigenwaves in the chiral medium. One is the right-handed circularly polarized (RCP, $+$) wave and the other is the left-handed circularly polarized (LCP, $-$) wave. The electromagnetic fields in the chiral medium can be expressed as [9]:

$$\mathbf{E} = \mathbf{E}_+ + \mathbf{E}_-, \quad \mathbf{H} = \mathbf{H}_+ + \mathbf{H}_-, \quad \mathbf{H}_\pm = \pm j\mathbf{E}_\pm/\eta \tag{2}$$

where $\eta = \sqrt{\mu\mu_0/\varepsilon\varepsilon_0}$ is the wave impedance in the chiral medium. According to the Maxwell's equations and the constitutive relations, we can get the wave equation of the electric field $\mathbf{E}_\pm$ propagating in the chiral medium:

$$\left(\nabla^2 + k_\pm^2\right)\mathbf{E}_\pm = 0 \tag{3}$$

where $k_\pm = n_\pm k_0$ are the wavenumbers of the two eigenwaves in the chiral medium, and $k_0 = \omega\sqrt{\mu_0\varepsilon_0}$ is the wavenumber in vacuum. $n_\pm$ are the indices of refraction for RCP and LCP waves, which are given by:

$$n_\pm = n \pm \kappa \tag{4}$$

where $n = \sqrt{\varepsilon\mu}$. From Equation (4), we can immediately find that the index of refraction for LCP or RCP wave can achieve negative refractive index, if $n < |\kappa|$. Thus, $|\kappa|$ should be large enough to overcome the magnitude of n to achieve negative $n_\pm$. Unlike conventional negative index structure designs [2, 3], the chiral negative index structure does not require simultaneously negative permittivity and negative permeability.

3. DESIGN AND SIMULATION OF MICROWAVE FREQUENCY BAND CHIRAL STRUCTURE

The structure of the proposed chiral medium is periodic, and one of the unit cells is shown in Figure 1. It is composed of L-shaped copper

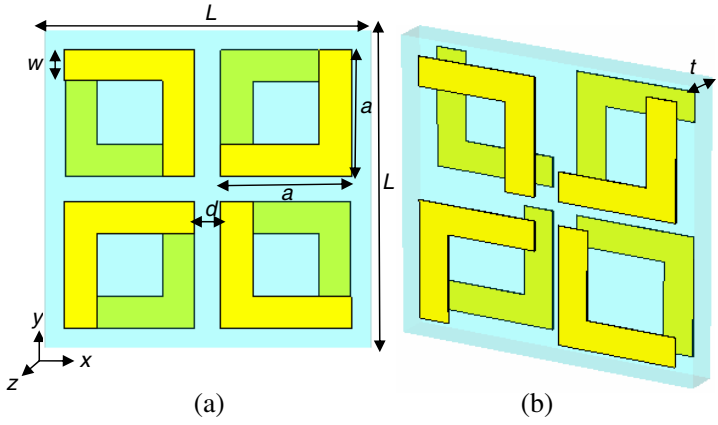

Figure 1. Schematics of L-shaped chiral negative refractive structure working in microwave frequency band. (a) Top view of the unit cell structure. (b) Perspective view of the unit cell structure.

foils ($\sigma = 5.8e7\,\mathrm{S/m}$) separated by a dielectric layer. Four pairs form a unit, and each pair rotates 0°, 90°, 180°, and 270° respectively for the requirement of fourfold rotational symmetry. The two layers of every pair are mutually twisted by 180° with respect to their central axes. The length, width, thickness, and distance interval of copper foils are given by $a = 6\,\mathrm{mm}$, $w = 1.5\,\mathrm{mm}$, $t_m = 0.036\,\mathrm{mm}$, and $d = 1\,\mathrm{mm}$. The L-shaped copper foils are patterned on a double side FR-4 board. The relative dielectric constant of the FR-4 board is 4.0 with a dielectric loss tangent of 0.025. The periodic constant of unit is $L = 15\,\mathrm{mm}$, and the thickness of dielectric layer is $t = 1.6\,\mathrm{mm}$. Numerical simulations are executed using a finite-element frequency-domain approach. A plane wave occurs along the negative z-direction and incidents normally onto surface plane of L-shaped structure. Periodic boundary condition is used in the direction perpendicular to the propagation direction. The overall unit structure has fourfold rotational symmetry, with no center of inversion, and no mirror planes. Hence, it is truly chiral.

Figure 2(a) shows the simulated transmission spectra for the LCP (T_{--}) and RCP (T_{++}) waves. Two resonance dips are observed at frequencies, $f = 12.6\,\mathrm{GHz}$ and $14.3\,\mathrm{GHz}$, in both T_{--} and T_{++} curves. At the resonances, the transmission spectra for the RCP (T_{++}) and LCP (T_{--}) waves are clearly different. Around the frequency of $12.6\,\mathrm{GHz}$, the transmission of LCP wave is 4–5 dB lower than that of the RCP wave. While around the frequency of $14.3\,\mathrm{GHz}$, the transmission of RCP wave is 12–13 dB lower than that of the LCP wave. Figure 2(b) shows that this structure has a large circular dichroism at the two resonances, which can be calculated by $\Delta = |T_{++}| - |T_{--}|$. Using the ellipticity angle $\eta = \frac{1}{2}\arcsin\frac{|T_{++}|^2 - |T_{--}|^2}{|T_{++}|^2 + |T_{--}|^2}$, and the polarization azimuth rotation angle $\theta = \frac{1}{2}[\arg(T_{++}) - \arg(T_{--})]$, we calculate the polarization changes in linear polarized wave incidents on the L-shaped structure. Figures 2(c) and 2(d) show the simulated results of the ellipticity angle η and polarization azimuth rotation angle θ of the transmitted wave, respectively. In the vicinity of the resonance frequencies of $12.6\,\mathrm{GHz}$ and $14.3\,\mathrm{GHz}$, the ellipticity angle and the polarization azimuth rotation angle respectively reach their maximum values. $\eta = 0$ corresponds to a pure optical activity effect, i.e., for the linear polarization incident wave, the transmitted wave will still be linear polarization but with a rotated angle θ. We observe the polarization rotation angle of $\theta = 40°$ with $\eta = 0$. Our chiral structure possesses huger pure polarization azimuth rotation angle compared with other reported microwave frequency band chiral structures: twisted rosettes structure [13, 27] (7° and 3°, respectively), U-shaped structure [31] (26°) and conjugated gammadion structure [46] (30°).

Using the retrieval procedure [13], we also calculate the effective

parameters κ, n_+, n_-, n, ε and μ from the simulated transmission and reflection spectra. Figure 3(a) presents the real parts of the relative permittivity ε and permeability μ for the L-shaped chiral structure. It is clear that the resonance around the frequency of 12.6 GHz is electric resonance and the resonance around the frequency of 14.3 GHz is magnetic resonance, which demonstrates that the resonance in Figure 2(a) at 12.6 GHz is caused by the electric resonance, and the resonance at 14.3 GHz is caused by the magnetic resonance. We also find that the permittivity and permeability are without simultaneously negative at the resonance. Figure 3(b) presents the real parts of the chiral parameter κ, the refractive index for RCP (n_+) and LCP (n_-)

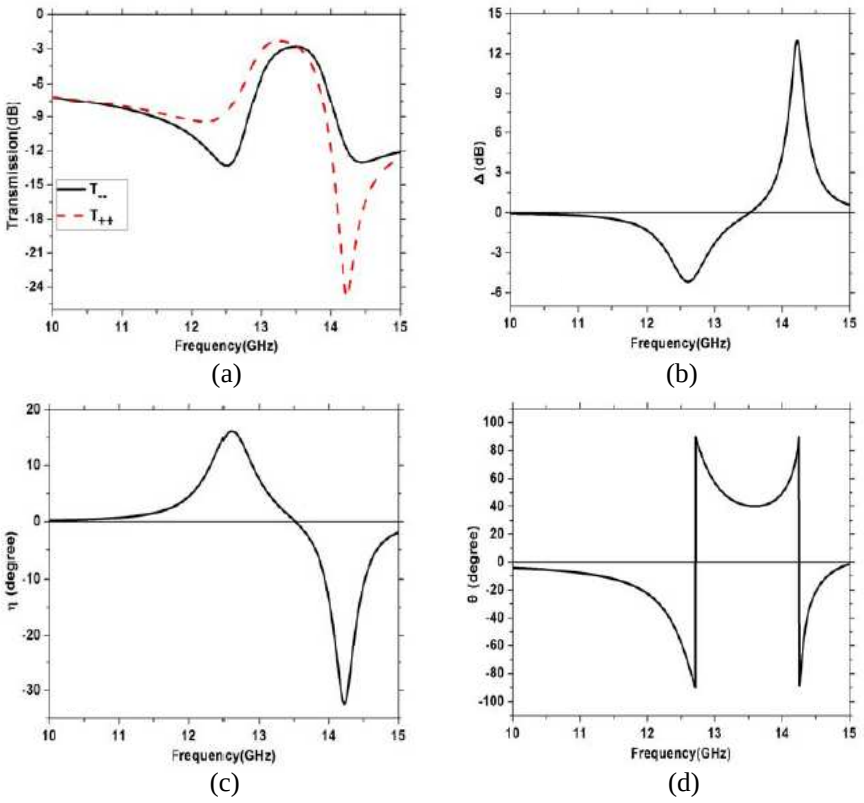

Figure 2. Simulated results for the microwave frequency band chiral structure. (a) The transmission spectra for LCP (T_{--}) and RCP (T_{++}) waves; (b) the circular dichroism; (c) the ellipticity angle η; (d) the polarization azimuth rotation angle θ.

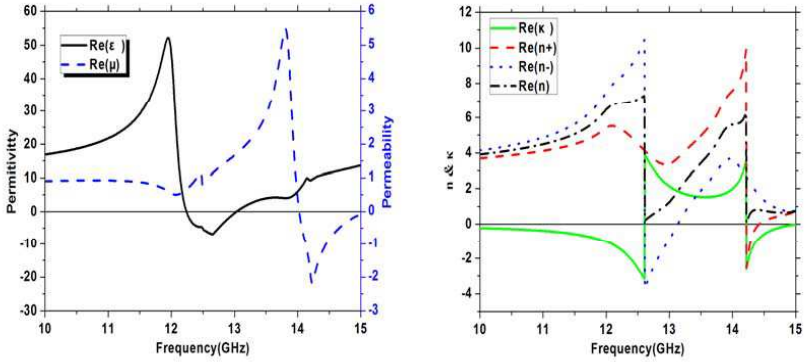

Figure 3. (a) The real part of the relative permittivity ε and permeability μ; (b) the real part of the chiral parameter κ, the refractive index for RCP (n_+) and LCP (n_-) waves, and the conventional definition of refractive n.

waves, and the conventional definition of refractive n. Note that around the two resonances, the chiral parameter reaches their maximum values. Due to the relation of $n_\pm = n \pm \kappa$, the large chiral parameter leads to $n_- < 0$ at frequency region $12.6 \sim 13.1$ GHz and $n_+ < 0$ at frequency region $14.3 \sim 14.5$ GHz, their maximum negative refractive indices are -3.2 and -2.5, respectively. The negative refractive index for RCP (n_+) and LCP (n_-) waves originates from the chiral parameter if we notice that n is positive through the entire frequency range from 10 GHz to 15 GHz. This structure may have many potential applications such as cloaking and subwavelength imaging.

In order to understand the mechanism of the resonances for the L-shaped chiral structure, we study the surface current distribution as shown in Figure 4. The solid arrows denote the surface current directions for the upper L-shaped layer, and the dashed arrows denote the surface current directions for the bottom L-shaped layer. Figure 4(a) shows that at the resonant frequency of 12.6 GHz, the surface currents on the top and bottom layer are parallel for the A and B, suggesting that the structure acts like an electric dipole at 12.6 GHz. That is the reason why the relative permittivity ε occurring resonance at 12.6 GHz. On the contrary, at 14.3 GHz, the surface currents on the two layers are antiparallel, and they form a current loop for the A and B, as illustrated in Figure 4(b). Moreover, the induced magnetic field component points to left, indicating that the structure acts like a magnetic dipole at 14.3 GHz. That results in resonance for the relative permeability μ at 14.3 GHz.

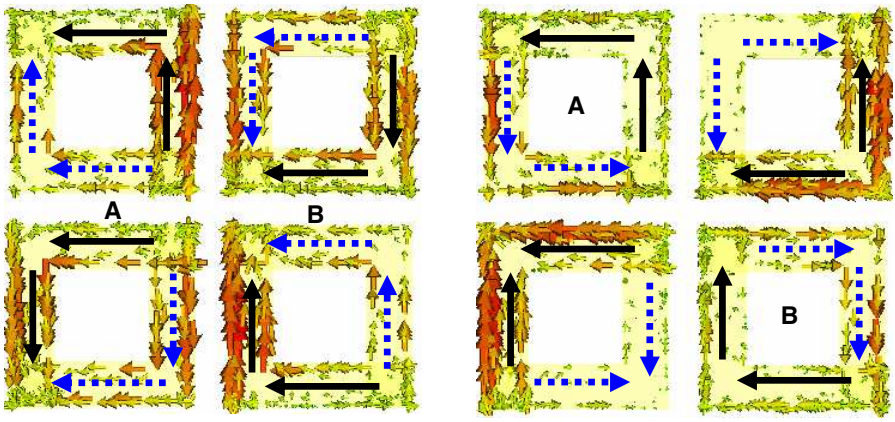

(a) $f = 12.6$ GHz (b) $f = 14.3$ GHz

Figure 4. The surface current distribution of the L-shaped chiral structure for the LCP wave incidence at (a) 12.6 GHz and (b) 14.3 GHz. The solid arrows denote the surface current directions for the upper L-shaped layer, and the dashed arrows denote the surface current directions for the bottom L-shaped layer.

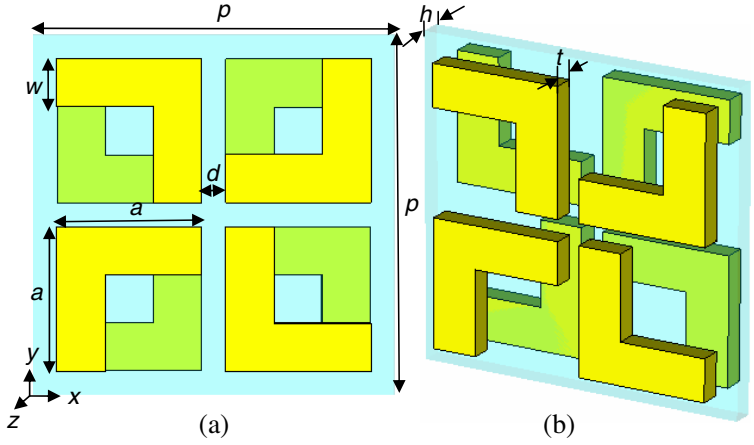

Figure 5. Schematics of L-shaped chiral negative refractive structure working in optical frequency band. (a) Top view of the unit cell structure. (b) Perspective view of the unit cell structure.

4. DESIGN AND SIMULATION OF OPTICAL FREQUENCY BAND CHIRAL STRUCTURE

Figure 5 shows the schematic of one unite cell of the L-shaped optical frequency band chiral structure. Periodic constant $p = 750\,\text{nm}$. The length, width, thickness and distance interval of metallic L-shape are $a = 300\,\text{nm}$, $w = 100\,\text{nm}$, $t = 50\,\text{nm}$ and $d = 50\,\text{nm}$. We choose gold as metallic material and use MgF_2 ($n = 1.38$) as dielectric layer. The thickness of dielectric layer is $h = 50\,\text{nm}$. In the simulation, the gold optical properties are handled with a frequency dependent Drude model with plasma frequency $\omega_p = 2\pi \times 2133\,\text{THz}$ and collision

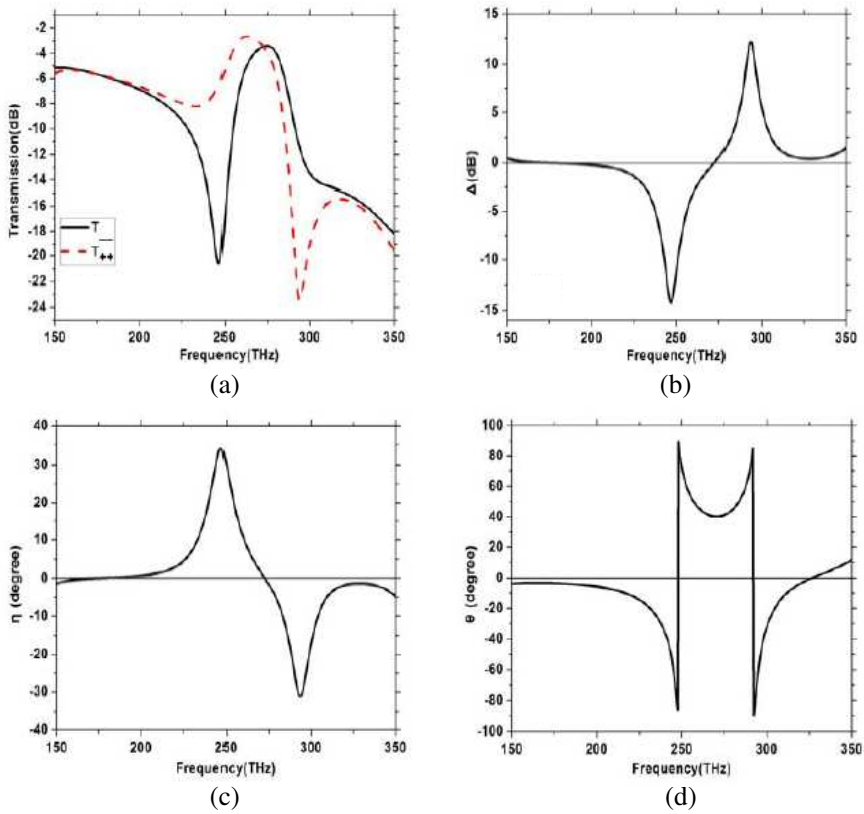

Figure 6. Simulated results for the optical frequency band chiral structure. (a) The transmission spectra for LCP and RCP waves; (b) the circular dichroism; (c) the ellipticity angle η; (d) the polarization azimuth rotation angle θ.

frequency $\omega_c = 2\pi \times 33\,\text{THz}$ [29]. A plane wave occurs along the negative z-direction and incidents normally onto surface plane of the structure. The periodic boundary condition is applied to the direction perpendicular to the propagation direction.

Firstly, we also calculate the transmission spectra of LCP (T_{--}) and RCP (T_{++}) waves, as shown in Figure 6(a). We can find obvious resonance dips around the frequencies of 247 THz and 292 THz. For the first resonance at 247 THz, the transmission dip for LCP (T_{--}) wave is much deeper than that for RCP (T_{++}) wave, which means the resonance for LCP wave is much stronger than RCP wave. While for the second resonance at 292 THz, the resonance for RCP wave is much stronger than LCP wave. Figure 6(b) shows that this optical frequency band chiral structure also has a large circular dichroism at the two resonances, so the structure has distinct optical property. The retrieved ellipticity angle η and polarization azimuth rotation angle θ also show that our structure has notable optical performance. In Figure 6(c), the ellipticity angle η reaches 34° at 247 THz, and is up to $-30°$ at 292 THz. While at the around two resonant frequencies, the polarization azimuth rotation angle θ reaches their maximum values (Figure 6(d)). At the frequency range between 247 THz and 292 THz, we gain a polarization rotation angle of 40° with $\eta = 0$, which is larger than the value reported in references [26, 29] (7° and 30°, respectively). It may have many potential applications such as perfect linear polarizer and half-wave plate.

In Figure 7(a), the real part of the chiral parameter κ can

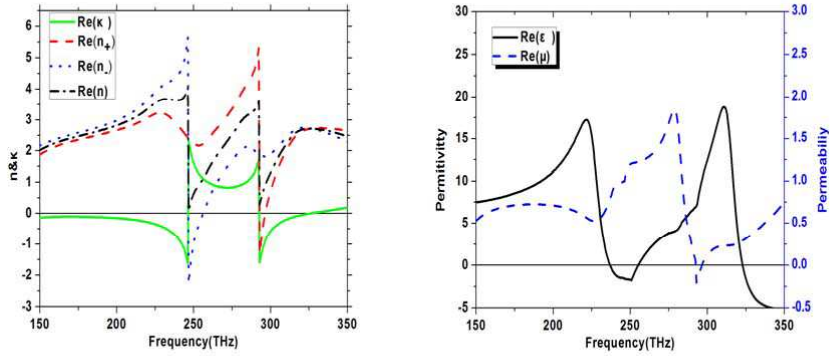

Figure 7. (a) The real part of the chiral parameter κ, the refractive index for RCP (n_+) and LCP (n_-) waves, and the conventional definition of refractive n; (b) the real part of the relative permittivity ε and permeability μ.

reach 2.3 and -1.6 around the resonance frequencies of 247 THz and 292 THz, respectively. Consequently, the refractive index of LCP (n_-) wave becomes negative between 247 THz and 256 THz, whereas the refractive index of RCP (n_+) wave becomes negative between 292 THz and 295 THz, and their maximum negative refractive indices can reach -2.2 and -1.3, respectively. The reason is that in the frequency range from 247 THz to 256 THz, the chiral parameter κ is positive and the value is bigger than refractive index n, leading to $n_- < 0$. Similarly, in the frequency range from 292 THz to 295 THz, the chiral parameter κ is negative and the absolute value is bigger than refractive index n, leading to $n_+ < 0$. In Figure 7(b), the ε is negative in the frequency range from 236 THz to 256 THz, while the μ is negative in the frequency range from 292 THz to 295 THz. There is no overlap region of negative ε and μ. For the traditional negative refractive medium [2, 3], this will not result in negative index. Therefore, the negative refractive index of LCP (RCP) wave is completely due to large chiral parameter κ.

5. CONCLUSION

In summary, the properties of L-shaped chiral negative refractive structure working in microwave frequency band and optical frequency band have been investigated by numerical simulation. The results show that the microwave frequency band chiral structure possesses giant optical activity and very large circular dichroism at 12.6 GHz and 14.3 GHz, and the refractive index of LCP (n_-) wave is negative from 12.6 GHz to 13.1 GHz, and the refractive index of RCP (n_+) wave is negative from 14.3 GHz to 14.5 GHz. While the optical frequency band chiral structure has strong optical activity and large circular dichroism at 247 THz and 292 THz, and n_- is negative from 247 THz to 256 THz and n_+ is negative from 292 THz to 295 THz. Especially, we observe a polarization rotation angle of 40° with $\eta = 0$ for the L-shaped chiral structure, which is larger than the value reported in bi-layer chiral negative refractive structure [13, 26, 27, 29, 31, 46]. The numerical simulations also show that the negative refractive index of the chiral structure is due to a large chiral parameter but dose not require simultaneously negative permittivity and negative permeability. The chiral structure has excellent optical properties, and there are potential applications in the optical functional materials and optical polarization devices. The geometry of the L-shaped chiral structure is simple and easy to fabricate, the microwave frequency band structure can be manufactured by PCB (Printed Circuit Board) and the optical frequency band structure can be fabricated by EBL (Electron Beam Lithography).

ACKNOWLEDGMENT

This work is supported by the National Natural Science Foundation of China (61078060), the Natural Science Foundation of Zhejiang Province, China (Y1091139), Ningbo Optoelectronic Materials and Devices Creative Team (2009B21007), and is partially sponsored by K. C. Wong Magna Fund in Ningbo University.

REFERENCES

1. Veselago, V. G., "The electrodynamics of substances with simultaneously negative values of ε and μ," *Sov. Phys. Usp.*, Vol. 10, No. 4, 509–514, 1968.
2. Smith, D. R., W. J. Padilla, D. C. Vier, S. C. Nemat-Nasser, and S. Schultz, "Composite medium with simultaneously negative permeability and permittivity," *Phys. Rev. Lett.*, Vol. 84, No. 18, 4184–4187, 2000.
3. Shelby, R. A., D. R. Smith, and S. Schultz, "Experimental verification of a negative index of refraction," *Science*, Vol. 292, 77–79, 2001.
4. Caloz, C. and T. Itoh, "Application of the transmission line theory of left-handed (LH) materials to the realization of a microstrip "LH line"," *IEEE Antennas and Propagation Society International Symposium*, Vol. 2, 412–415, 2002.
5. Eleftheriades, G. V., A. K. Iyer, and P. C. Kremer, "Planar negative refractive index media using periodically L-C loaded transmission lines," *IEEE. Trans. Microwave Theory and Tech.*, Vol. 50, No. 12, 2702–2712, 2002.
6. Cubukcu, E., K. Aydin, E. Ozbay, S. Foteinopoulou, and C. M. Soukoulis, "Electromagnetic waves: Negative refraction by photonic crystals," *Nature*, Vol. 423, 604–605, 2003.
7. Parimi, P. V., W. T. Lu, P. Vodo, and S. Srinivas, "Photonic crystals: Imaging by flat lens using negative refraction," *Nature*, Vol. 426, 404–406, 2003.
8. Tretyakov, S., I. Nefedov, A. Sihvola, S. Maslovski, and C. Simovski, "Waves and energy in chiral nihility," *Journal of Electromagnetic Waves and Applications*, Vol. 17, No. 5, 695–706, 2003.
9. Tretyakov, S., A. Sihvola, and L. Jylha, "Backward-wave regime and negative refraction in chiral composites," *Photonics Nanostruct. Fundam. Appl.*, Vol. 3, Nos. 2–3, 107–115, 2005.

10. Pendry, J. B., "A chiral route to negative refraction," *Science*, Vol. 306, 1353–1355, 2004.
11. Mackay, T. G., "Plane waves with negative phase velocity in isotropic chiral mediums," *Microwave Opt. Tech. Lett.*, Vol. 45, No. 2, 120–121, 2005.
12. Zhou, J., J. Dong, B. Wang, T. Koschny, M. Kafesaki, and C. M. Soukoulis, "Negative refractive index due to chirality," *Phys. Rev. B*, Vol. 79, 121104, 2009.
13. Plum, E., J. Zhou, J. Dong, V. A. Fedotov, T. Koschny, C. M. Soukoulis, and N. I. Zheludev, "Metamaterial with negative index due to chirality," *Phys. Rev. B*, Vol. 79, 035407, 2009.
14. Zhang, S., Y. Park, J. Li, X. Lu, W. Zhang, and X. Zhang, "Negative refractive index in chiral metamaterials," *Phys. Rev. Lett.*, Vol. 102, 023901, 2009.
15. Dong, J. and C. Xu, "Characteristics of guided modes in planar chiral nihility meta-material waveguides," *Progress In Electromagnetics Research B*, Vol. 14, 107–126, 2009.
16. Dong, J. F., "Surface wave modes in chiral negative refraction grounded slab waveguides," *Progress In Electromagnetics Research*, Vol. 95, 153–166, 2009.
17. Dong, J., "Exotic characteristics of power propagation in the chiral nihility fiber," *Progress In Electromagnetics Research*, Vol. 99, 163–178, 2009.
18. Dong, J., J. Li, and F.-Q. Yang, "Guided modes in the four-layer slab waveguide containing chiral nihility core," *Progress In Electromagnetics Research*, Vol. 112, 241–255, 2011.
19. Rahim, T., M. J. Mughal, and Q. A. Naqvi, "PEMC paraboloidal reflector in chiral medium supporting positive phase velocity and negative phase velocity simultaneously," *Progress In Electromagnetics Research Letters*, Vol. 10, 77–86, 2009.
20. Ahmed, S. and Q. A. Naqvi, "Electromagnetic scattering from a chiral-coated nihility cylinder," *Progress In Electromagnetics Research Letters*, Vol. 18, 41–50, 2010.
21. Mehmood, M. Q., M. J. Mughal, and T. Rahim, "Focal region fields of cassegrain system placed in homogeneous chiral medium," *Progress In Electromagnetics Research B*, Vol. 21, 329–346, 2010.
22. Rahim, T. and M. J. Mughal, "Spherical reflector in chiral medium supporting positive phase velocity and negative phase velocity simultaneously," *Journal of Electromagnetic Waves and Applications*, Vol. 23, No. 11–12, 1665–1673, 2009.
23. Naqvi, Q. A., "Fractional dual solutions in grounded chiral nihility

slab and their effect on outside field," *Journal of Electromagnetic Waves and Applications,* Vol. 23, No. 5–6, 773–784, 2009.

24. Naqvi, A., A. Hussain, and Q. A. Naqvi, "Waves in fractional dual planar waveguides containing chiral nihility metamaterial," *Journal of Electromagnetic Waves and Applications*, Vol. 24, No. 11–12, 1575–1586, 2010.
25. Tuz, V. R. and C.-W. Qiu, "Semi-infinite chiral nihility photonics: Parametric dependence, wave tunneling and rejection," *Progress In Electromagnetics Research*, Vol. 103, 139–152, 2010.
26. Dong, J., J. Zhou, T. Koschny, and C. Soukoulis, "Bi-layer cross chiral structure with strong optical activity and negative refractive index," *Optics Express*, Vol. 17, No. 16, 14172–14179, 2009.
27. Rogacheva, A. V., V. A. Fedotov, A. S. Schwanecke, and N. I. Zheludev, "Giant gyrotropy due to electromagnetic-field coupling in a bilayered chiral structure," *Phys. Rev. Lett.*, Vol. 97, 177401, 2006.
28. Plum, E., V. A. Fedotov, A. S. Schwanecke, N. I. Zheludev, and Y. Chen, "Giant optical gyrotropy due to electromagnetic coupling," *Appl. Phys. Lett.*, Vol. 90, No. 22, 223113, 2007.
29. Decker, M., R. Zhao, C. M. Soukoulis, S. Linden, and M. Wegener, "Twisted split-ring-resonator photonic metamaterial with huge optical activity," *Opt. Lett.*, Vol. 35, No. 10, 1593–1595, 2010.
30. Xiong, X., W. Sun, Y. Bao, M. Wang, R. Peng, C. Sun, X. Lu, J. Shao, Z. Feng, and N. Ming, "Construction of a chiral metamaterial with a U-shaped resonator assembly," *Phys. Rev. B*, Vol. 81, 075119, 2010.
31. Li, Z., R. Zhao, T. Koschny, M. Kafesaki, K. B. Alici, E. Colak, H. Caglayan, E. Ozbay, and C. M. Soukoulis, "Chiral metamaterials with negative refractive index based on four "U" split ring resonators," *Appl. Phys. Lett.*, Vol. 97, 081901, 2010.
32. Wu, Z., B. Q. Zeng, and S. Zhong, "A double-layer chiral metamaterial with negative index," *Journal of Electromagnetic Waves and Applications*, Vol. 24, No. 7, 983–992, 2010.
33. Wu, Z., J. Zhu, M. Jia, H. Lu, and B. Zeng, "A double-layer metamaterial with negative refractive index originating from chiral configuration," *Microwave Opt. Tech. Lett.*, Vol. 53, No. 1, 163–166, 2011.
34. Ye, Y. and S. He, "90° polarization rotator using a bilayered chiral metamaterial with giant optical activity," *Appl. Phys. Lett.*, Vol. 96, 203501, 2010.
35. Cheng, Q., W. X. Jiang, and T. J. Cui, "Investigations of the

electromagnetic properties of three-dimensional arbitrarily-shaped cloaks," *Progress In Electromagnetics Research*, Vol. 94, 105–117, 2009.

36. Luo, Y., J. Zhang, H. Chen, B.-I. Wu, and L.-X. Ran, "Wave and ray analysis of a type of cloak exhibiting magnified and shifted scattering effect," *Progress In Electromagnetics Research*, Vol. 95, 167–178, 2009.
37. Han, T. C., C.-W. Qiu, and X. H. Tang, "Creating rigorous open cloaks," *Journal of Electromagnetic Waves and Applications*, Vol. 24, No. 13, 1839–1847, 2010.
38. Jin, Y. and S. He, "Focusing by a slab of chiral medium," *Optics Express*, Vol. 13, No. 13, 4974–4979, 2005.
39. Monzon, C. and D. W. Forester, "Negative refraction and focusing of circularly polarized waves in optically active media," *Phys. Rev. Lett.*, Vol. 95, 123904, 2005.
40. Cheng, Q., H. F. Ma, and T. J. Cui, "A complementary lens based on broadband metamaterials," *Journal of Electromagnetic Waves and Applications*, Vol. 24, No. 1, 93–101, 2010.
41. Illahi, A. and Q. A. Naqvi, "Study of focusing of electromagnetic waves reflected by a PEMC backed chiral nihility reflector using Maslov's method," *Journal of Electromagnetic Waves and Applications*, Vol. 23, No. 7, 863–873, 2009.
42. Liu, H. and S. He, "Near-field optical storage system using a solid immersion lens with a left-handed material slab," *Optics Express*, Vol. 12, No. 20, 4835–4840, 2004.
43. Navarro-Cia, M., M. Beruete, F. J. Falcone, M. Sorolla, and I. Campillo, "Polarization-tunable negative or positive refraction in self-complementariness-based extraordinary transmission prism," *Progress In Electromagnetics Research*, Vol. 103, 101–114, 2010.
44. Wang, J., S. Qu, H. Ma, Y. Yang, X. Wu, Z. Xu, and M. Hao, "Wide-angle polarization-independent planar left-handed metamaterials based on dielectric resonators," *Progress In Electromagnetics Research B*, Vol. 12, 243–258, 2009.
45. Lindell, I. V., A. H. Sihvola, S. A. Tretyakov, and A. J. Viitanen, *Electromagnetic Waves in Chiral and Bi-isotropic Media*, Artech House, Boston, 1994.
46. Zhao, R., L. Zhang, J. Zhou, T. Koschny, and C. M. Soukoulis, "Conjugated gammadion chiral metamaterial with uniaxial optical activity and negative refractive index," *Phys. Rev. B*, Vol. 83, 035105, 2010.